SCIENTIFIC REPORTS

OPEN

Low-temperature synthesis of high-ordered anatase TiO₂ nanotube array films coated with exposed {001} nanofacets

Jie Ding[1], Zhennan Huang[1,2], Jihao Zhu[3], Shengzhong Kou[2], Xiaobin Zhang[1] & Hangsheng Yang[1]

High-ordered anatase TiO₂ nanotube array films coated with exposed high-reactive {001} nanofacets were fabricated by a modified hydrothermal method using amorphous anodic TiO₂ nanotube arrays (ATONAs) as starting materials. It was found that the reaction between gas phase HF and solid ATONAs played a key role in the transformation process from amorphous to anatase TiO₂, and the TiO₂ tubular structure kept unchanged during the surface modification with an exposed {001} facets up to 76.5%, which could be attributed to the low reaction temperature of 130 °C. Our study provided a novel route for the facile preparation of {001} facets exposed anatase TiO₂.

(1) Anatase TiO₂ nanotube array films coated with exposed {001} nanofacets have been synthesized by a modified hydrothermal method.
(2) Anatase TiO₂ with 76.5% of exposed {001} facets was achieved at temperature as low as 130 °C.
(3) A novel reaction route between HF gas and solid ATONAs played a key role.
(4) The transformation depended on solid state atomic rearrangement.

Among the three main titanium dioxide (TiO₂) polymorphs, anatase TiO₂ has attracted much attention because of its unique electronic, optical and catalytic properties[1–3], which showed various applications such as photocatalysis, photovoltaics, drug delivery, hydrogen production and lithium ion batteries[4–7]. Recently, the synthesis and application of anatase TiO₂ with exposed {001} facets have been a hot topic[8]. Both theoretical and experimental studies revealed that the exposed (001) surfaces showed much higher chemical activities than the (101) surfaces in anatase TiO₂ crystals[8–10]. Therefore, it is desirable to prepare TiO₂ crystals with more reactive {001} facets exposed. Hydrothermal synthesis with F⁻ has been proven to be the most frequently used and the most effective method[8–13]. The main procedures for the exposal of {001} planes of anatase TiO₂ included two steps: (i) the preparation of low surface energy {001} planes by terminating the dangling bonds with F⁻, at this stage, the photocatalytic activity of the TiO₂ is still low; (ii) the removal of surface F⁻ by 600 °C annealing which produced F⁻ free exposed {001} planes. Note that the first step is essential for the exposal of {001} nanofacets. Up to now, a reaction temperature at least 200 °C is necessary for the hydrothermal preparation of anatase TiO₂ with exposed {001} facets[8–13].

Herein, we found that by using a modified hydrothermal method, which avoided the direct contact of ATONAs with HF solution[13–15], thus the reaction between gas phase HF (but not acid HF solution) and solid ATONAs played a key role in the transformation process from amorphous to anatase TiO₂, and

[1]State Key Laboratory of Silicon Materials, School of Materials Science and Engineering, Zhejiang University, Zheda Road 38, Hangzhou 310027, China. [2]State Key Laboratory of Advanced Processing and Recycling of Nonferrous Metals, Lanzhou University of Technology, Lanzhou 730050, China. [3]The Second Institute of Oceanography, State Oceanic Administration, Baochubei Road 36, Hangzhou 310012, China. Correspondence and requests for materials should be addressed to H.Y. (email: hsyang@zju.edu.cn)
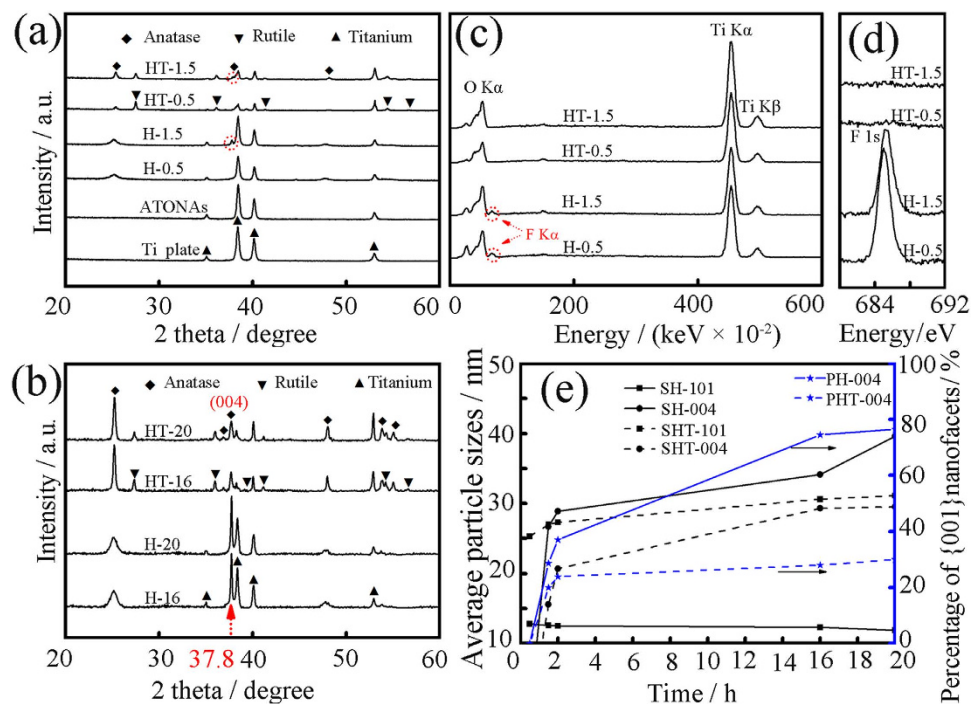
Figure 1. (**a**) and (**b**) XRD patterns of the samples before and after post annealing. The red dot circle is the location of (004) planes of the anatase TiO_2. (**c**) EDS patterns of sample before (H-0.5 and H-1.5) and after (HT-0.5 and HT-1.5) post annealing, the red dot circle is the position of F Kα. (**d**) XPS spectra of two samples before and after post annealing, which clearly showed that the surface F⁻ ions were removed by annealing. (**e**) Structural information of the synthesized samples. SH-101 and SH-004: the average particle sizes calculated from the FWHM of (101) and (004) peak for samples before post annealing; SHT-101 and SHT-004: the average particle sizes calculated from the FWHM of (101) and (004) peak for samples after annealing; PH-004 and PHT-004: the percentage of exposed {001} nanofacets before and after annealing.

TiO₂ nanotube array films with exposed {001} facets up to 76.5% was successfully prepared at reaction temperature as low as 130 °C. After the surface F⁻ ions were removed by 2 h of 600 °C annealing[8,13,16], the obtained F⁻ free TiO₂ films with exposed {001} nanofacets showed much better photocatalytic activities than the original ATONAs for methyl orange (MO) degradation.

Results

Figure 1a,b shows the XRD patterns of the as-synthesized samples with different preparation conditions. For ATONAs, only diffraction peaks of titanium were detected, indicating that the as grown ATONAs have amorphous structure[17]. After hydrothermal treatment, broad diffraction peaks at 25.3°, 37.8°, 48.2°, 53.9° and 55.2° were observed, which can be indexed to the (101), (004), (200), (105) and (211) reflections of anatase TiO₂, and the diffraction peak intensities at 25.3° and 37.8° increased with preparation time, indicating the nucleation and growth of anatase TiO₂ during 130 °C hydrothermal treatment (the XRD patterns of samples for 1.5 h and 2 h were shown in Fig. S1 in Supporting Information). Note that, the appearance of strong peak at 37.8°, which was attributed to (004) planes of anatase TiO₂, suggested the presence of exposed {001} nanofacets[18]. Especially for H-16 and H-20 (Fig. 1b), the exposed {001} planes was estimated to be as high as 74.5% and 76.5%, respectively[19]. The EDS spectra in Fig. 1c indicated that the surface F⁻ ions were completely removed by 600 °C annealing[8,13,16]. XPS measurement also confirmed the successful removal of the surface F⁻ species, as shown in Fig. 1d. At the same time, diffraction peaks attributed to {101} planes sharpened, while the (004) peak at 37.8° weakened slightly, indicating that the loss of terminated F⁻ preferred the exposal of {101} planes. The average grain size estimated from FWHM of diffraction peaks at 25.3° and 37.8° was 12.2 nm and 34.1 nm for H-16, and 30.6 nm and 29.3 nm for HT-16, respectively as shown in Fig. 1e. By the way, the post annealing also induced the formation of rutile nanoparticles, as a result, diffraction peaks of 27.5°, 36.1°, 39.3° and 54.3° appeared[20,21].

Figure 2 shows SEM images of samples prepared under different conditions. The inset of Fig. 2a is SEM image showing the morphology of the as-prepared ATONAs, which were highly ordered and were grown vertically to the titanium substrate. Figure 2a is the ATONAs after 0.5 h hydrothermal treatment, the tubular structure was maintained with small particles coated on the surface (~8 nm estimated from the FWHM of peak at 25.3°). Even the hydrothermal treatment time increased to 20 h, the tubular structure
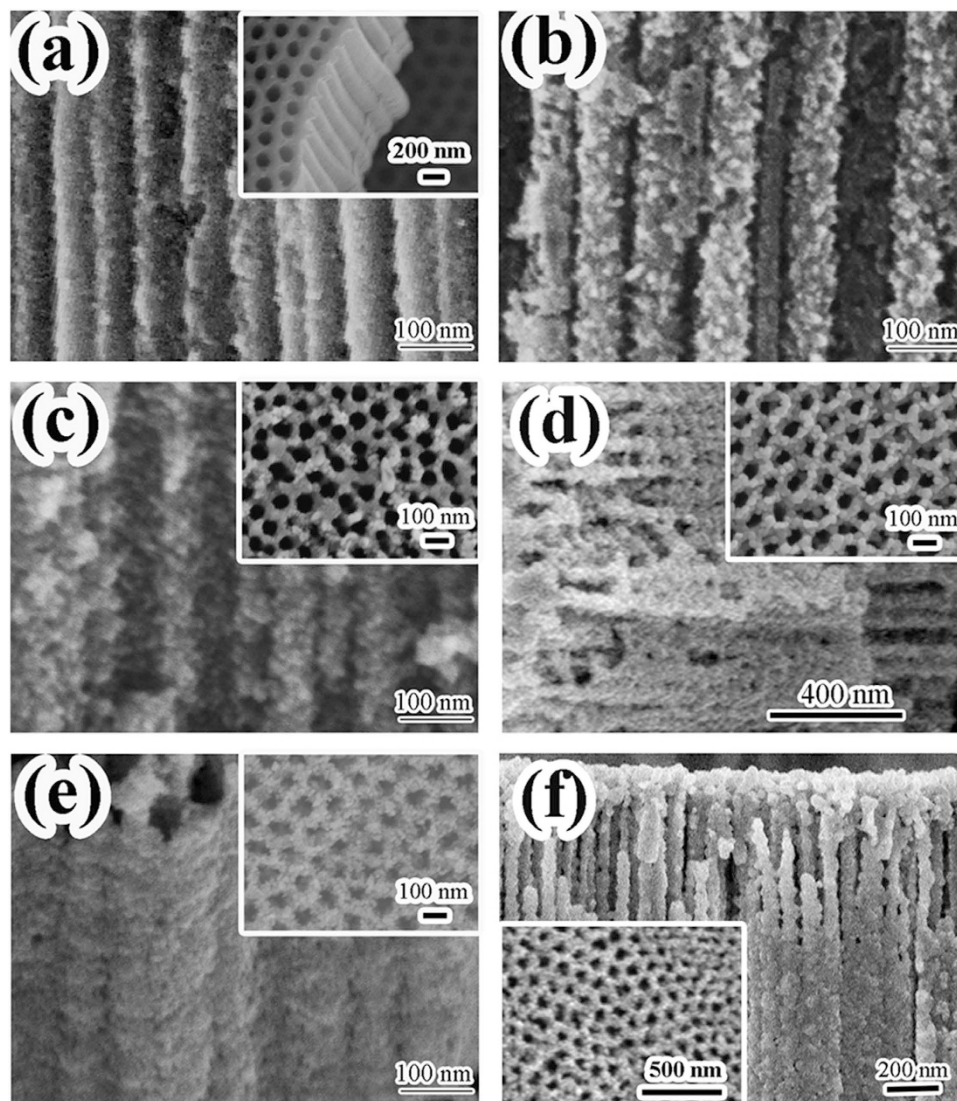
Figure 2. Typical SEM images of the samples: (**a**) H-0.5, (**b**) HT-0.5, (**c**) H-16, (**d**) HT-16, (**e**) H-20, (**f**) HT-20. The inset in (**a**) is as-prepared ATONAs, and other insets are morphology of film surface. And their low-magnification images are represented in ESI.

still kept unchanged as the cross section image shown in Fig. 2e. Amazingly, after 600 °C annealing, the surface coated nanoparticles grew up to be nanofacet like grains (insets of Fig. 2d,f), and the tubular structure was still maintained as shown in Fig. 2b,d,f, which provided an extremely large surface area compared to the normal TiO_2 films (low-magnification SEM images were shown in Figs. S2 to S6).

Figure 3a shows SEM image of nanoparticles with truncated bipyramidal or trapezoidal shapes and even some with cubic morphology of anatase TiO_2 coated on the surface of HT-2, which could be attributed to different degree of truncated octahedral. Figure 3b shows typical TEM image of some nanoparticles, which have regular facet-like geometry with exposed flat square[22]. All SEM and TEM images indicated the successful exposal of F^- free (004) planes after annealing[8]. Figure 1e summarized the grain size and the evaluation of percentage of exposed {001} planes, according to early estimation method[19,23,24], TiO_2 with exposed {001} facets up to 76.5% was successfully prepared.

Figure 4a shows the HRTEM image of H-2 sample, nanoparticles with grain size in the orders of several nanometers could be observed, the crystal lattice with a spacing of 0.235 nm (004), and 0.35 nm (101) confirmed the anatase TiO_2 nanoparticles[24]. Moreover, the observed (004) planes are parallel to the particle surface, which presented direct evidence for the existence of {001} exposed nanofacets. Evidently, the amorphous ATONAs partially transformed into anatase TiO_2 with exposed {001} nano-facets by hydrothermal treatment at 130 °C. Figure 4b is a typical HRTEM image of HT-2, in this selected observation window, almost all grains had spacing of 0.235 nm (parallel to the grain surface); indicated the high percentage of exposed {001} planes. By the way, a rutile TiO_2 grain with a spacing of 0.229 nm
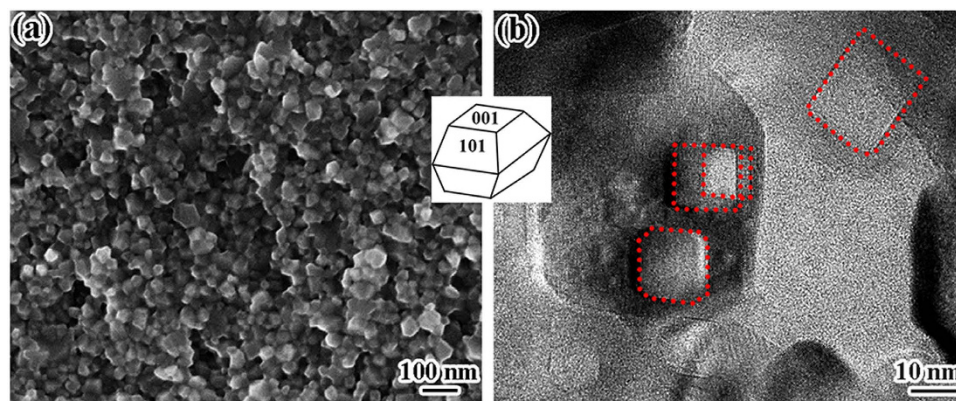
Figure 3. (**a**) SEM and (**b**) TEM image of HT-2. The inset is a model of equilibrium shape of anatase TiO$_2$ with exposed {101} and {001}.
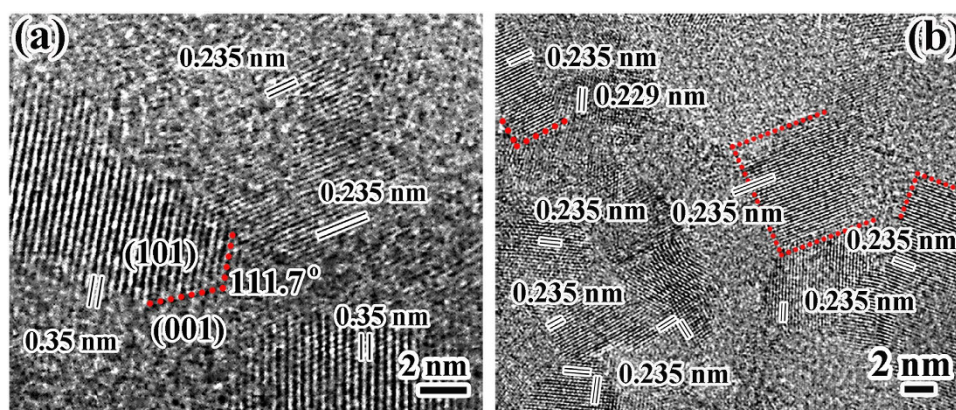

Figure 4. HRTEM images of (**a**) H-2 and (**b**) HT-2. The 0.235 nm and 0.35 nm are the distances between (004) planes and (101) plane of anatse TiO$_2$, respectively. The 111.7° is the angle between (004) plane and (101) plane of anatase TiO$_2$.

belonging to (200) planes was also detected, consistent with XRD results shown in Fig. 1. HRTEM images of HT-20 were shown in Fig. S7.

Discussion

Normally, anatase TiO$_2$ grains are dominated by {101} facets rather than {001} facets, the latter is more active but with high surface energy[25–29]. When the surface was terminated with F$^-$, the expose of {001} is energetically preferable to {101}, and this was proven theoretically and experimentally by using hydrothermal method[8–10], by which the Ti precursors were directly immersed into F$^-$/HF containing solutions[30]. A dissolution-precipitation or dissolution-recrystallization process was proposed to describe the transformation from {101} to {001} facets[31–33]. Here we modified the hydrothermal method by separating the ATONAs from the acid HF solution[30], accordingly, the reaction between gas phase HF and solid ATONAs becomes the only route for the transformation from amorphous to anatase TiO$_2$. From the XRD spectra shown in Fig. 1, a low temperature of 130 °C was enough to induce this transformation. This could be attributed to the use of amorphous TiO$_2$ as starting materials, which reduced the activation energy for atom rearrangement. The tubular structure of ATONAs was kept unchanged after hydrothermal treatment, which provided additional evidence that this transformation could not be explained through dissolution-precipitation or dissolution-recrystallization process, which destroyed the initial tubular structure[31–33]. The driving force for this transformation could be the surface energy change caused by F$^-$ termination, and {001} nanofacets were preferred finally[8–14]. From literature, the solid state transformation via atomic rearrangement in amorphous matrix is frequently proposed[34,35]. And the synthesis of anatase TiO$_2$ with exposed {001} facets by heat treatment (450 °C) using amorphous ATONAs as starting materials was achieved[13,16]. Here we demonstrated that a solid-state phase transformation from TiO$_2$ {101} to {001} facets could be achieved at a low temperature of 130 °C.

After the surface F$^-$ ions were removed by 600 °C post annealing, F$^-$ free {001} facets with high reactivity were achieved. Figure 5a shows the photocatalytic activities of ATONAs, HT-0.5, HT-1.5, HT-16,
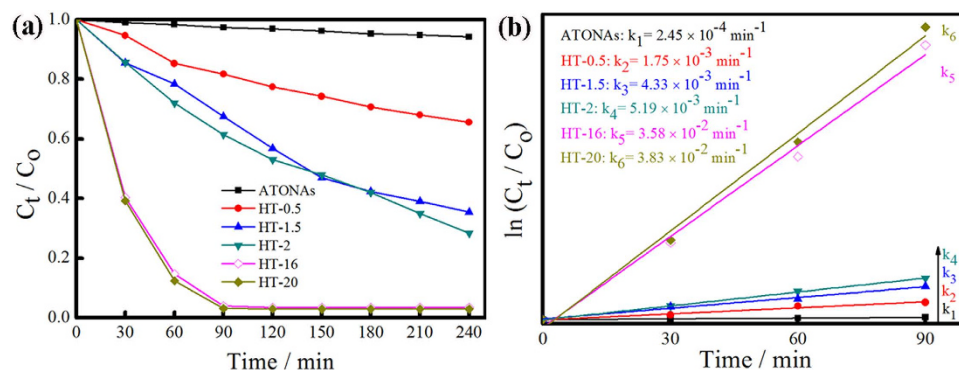
Figure 5. Photocatalytic activities of ATONAs, HT-0.5, HT-1.5, HT-2, HT-16, and HT-20 (**a**), and their corresponding pseudo-first-order kinetics (**b**).

and HT-20, respectively. The corresponding degradation efficiency increased with the percentage of {001} nanofacets, and more than 97% of MO could be removed in 90 min over HT-16 and HT-20. According to Langmuir-Hinshelwood model[36], the reaction rate coefficient k of HT-20 ($k_6 = 3.83 \times 10^{-2}$ min^{-1}) is 150 times higher than that of ATONAs ($k_1 = 2.45 \times 10^{-4}$ min^{-1}) (Fig. 5b), which demonstrated the excellent photocatalytic activities of TiO$_2$ nanotube array films with exposed {001} nanofacets obtained in this study, coincided well with earlier reports[13,15].

Conclusions

In summary, anatase TiO$_2$ nanotube array films with exposed {001} nanofacets were successfully prepared by a modified low-temperature hydrothermal method at 130 °C. The novel reaction route between gas phase HF and solid ATONAs was demonstrated which played a key role for the solid state transformation process from amorphous to anatase TiO$_2$, after the surface dangling bonds were terminated with F$^-$ ions, {001} facets became energetically favored. F$^-$ free {001} facets with high reactivity could be achieved via 600 °C post annealing. The prepared anatase TiO$_2$ nanotube array films with exposed {001} nanofacets exhibited enhanced photocatalytic activity for methyl orange (MO) degradation under ultraviolet light (UV), which could be attributed to the improvement of charge separation derived from the synergy effect between {001} and {101} facets.

Methods

Preparation of well-aligned anodic TiO$_2$ nanotubes (ATONAs). All reagents (Sinopharm, analytical grade, Shanghai, China) were used without further purification. Well-aligned ATONAs on a Ti substrate were fabricated via traditional electrochemical anodization[37]. Briefly, the anodic growth was conducted using a home-made two electrode electrochemical cell under a constant voltage of 40 V at room temperature, titanium plates (Ti, 90 mm × 40 mm × 0.2 mm, 99.9% purity, Baoji, Shanxi, China) were used as working electrode and a graphite plate as the counter electrode, the electrolyte was composed of 3 wt% NH$_4$F and 0.5 v% H$_2$O dissolved in the ethylene glycol. The obtained well-aligned ATONAs were rinsed with ethylene glycol and ethanol to remove the residual electrolyte solution followed by drying at 80 °C for later use (inset of Fig. 2a).

Exposing of {001} nanofacets. The well-aligned ATONAs were treated at 130 °C in an autoclave. In a typical experiment, 6 ml of hydrofluoric acid solution with pH = 3 was transferred to a Teflon-lined autoclave (capacity: 25 mL), then the as-synthesized ATONAs , which were cut into 2 cm × 2 cm dices, were fixed by Teflon holders 1 cm above the solution to avoid dipping the ATONAs into the solution. Then, the autoclave was sealed and heated at 130 °C for 0.5 h to 20 h. After the autoclave was cooled down to room temperature, the products were washed with ethylene glycol, ethanol and deionized water, and then dried in an oven at 80 °C for 0.5 h, the samples were labeled as H-t (where t stood for the hydrothermal time). Then, samples were heated at 600 °C for 2 h in air with a heating rate of 2°/min to obtain {001} nanofacets exposed films, and the final samples were labeled as HT-t.

Characterization. X-ray diffraction (XRD) patterns were recorded on a Philips XD-98 X-ray diffractometer with Cu Kα radiation (λ = 0.15406 nm). The morphology of the samples was characterized by A ZEISS ULTRA 55 scanning electron microscopy (SEM) equipped with energy dispersive spectrometer (EDS) and transmission microscopy (TEM, FEI Tecnai G^2 F20 S-TWIN, FEI Inc., America). X-ray photoelectron spectroscopy (XPS) data were obtained using a Thermo ESCALAB 250Xi (Thermo Fisher Scientific), the X-ray source was an Al Kα radiation, and all binding energies were referenced to the 284.8 eV C1s.

Photocatalytic activity.   The photocatalytic activities were evaluated by degrading the methyl orange (MO, 0.15 mg/L) as the model organic pollutants in aqueous solutions, three plates of {001} exposed TiO_2 films (size: 2 cm × 2 cm, TiO_2 weight: ca. 1.8 mg) were dipped in 30 mL of MO solution and then were irradiated by a 125 W mercury lamp which irradiated the light of 365 nm. Before irradiation, the system was put in a darkroom for 0.5 h with magnetic stirring to ensure adsorption and desorption equilibrium between the samples and organic molecules. The photodegradation experiments were performed in an open quartz vessel under continuously stirring. During degradation, 2 mL of MO were taken every 30 min and the concentration of MO was measured by UV-3600 spectrophotometer (Shimadzu, Japan) at 463 nm[38]. The influence of sampling was compensated in degradation efficiency calculation.

References

1. Burda, C. *et al.* Enhanced nitrogen doping in TiO_2 nanoparticles. *Nano Lett.* **3,** 1094–1051 (2003).
2. Chatterjee, D. & Dasgupta, S. Visible light induced photocatalytic degradation of organic pollutants. J. *Photochem. Photobiol. C* **6,** 186–205 (2005).
3. Chen, X. B. & Mao, S. S. Titanium dioxide nanomaterials: synthesis, properties, modifications, and applications. *Chem. Rev.* **107,** 2891–2959 (2007).
4. Fujishima, A. & Honda, K. Electrochemical photolysis of water at a semiconductor electrode. *Nature* **238,** 37–38 (1972).
5. Han, H. *et al.* Dominant factors governing the rate capability of a TiO_2 nanotube anode for high power lithium ion batteries. *ACS Nano* **6,** 8308–8315 (2012).
6. Habisreutinger, S. N., Schmidt-Mende, L. & Stolarczyk, J. K. Photocatalytic reduction of CO_2 on TiO_2 and other semiconductors. *Angew. Chem. Int. Ed.* **52,** 7372–7408 (2013).
7. Sarkar, D., Ghosh, C. K., Mukherjee, S. & Kalyan, K. C. Three dimensional Ag_2O/TiO_2 type-II (p-n) nanoheterojunctions for superior photocatalytic activity. *ACS Appl. Mater. Interfaces* **5,** 331–337 (2013).
8. Yang, H. G. *et al.* Anatase TiO_2 single crystals with a large percentage of reactive facets. *Nature* **453,** 638–641 (2008).
9. Pan, X. Y., Zhang, N., Fu, X. Z. & Xu, Y. J. Selective oxidation of benzyl over TiO_2 nanosheets with exposed {001} facets: catalyst deactivation and regeneration. *Appl. Catal. B* **453,** 181–187 (2013).
10. Roy, N., Sohn, Y. & Pradhan, D. Synergy of low-energy {101} and high-energy {001} TiO_2 crystal facets for enhanced photocatalysis. *ACS Nano* **7,** 2532–2540 (2013).
11. Wen, C. Z. *et al.* Synthesis of micro-sized titanium dioxide nanosheets wholly exposed with high-energy {001} and {100} facets. *Chem. Commun.* **47,** 4400–4402 (2011).
12. Ong, W. J., Tan, L. L., Chai, S. P., Yong, S. T. & Mohamed, A. R. Highly reactive {001} facets TiO_2–based composites: synthesis, formation mechanism and characterization. *Nanoscale* **6,** 1946–2008 (2014).
13. Liao, Y. L. *et al.* Activating the single-crystal TiO_2 nanoparticle film with exposed {001} facets. *ACS Appl. Mater. Interfaces* **5,** 6463–6466 (2013).
14. Wang, X. N. *et al.* Synthesis of anatase TiO_2 tubular structures microcrystallites with a high percentage of {001} facets by a simple one-step hydrothermal template process. *Chem. Eur. J.* **16,** 7106–7109 (2010).
15. Gao, Z. H. *et al.* Fabrication, characterization, and photocatalytic properties of anatase TiO_2 nanoplates with exposed {001} facets. *J. Nanopart. Res.* **16,** 1–9 (2014).
16. Liu, B. & Aydil, E. S. Anatase TiO_2 films with reactive {001} facets on transparent conductive substrate. *Chem. Commun.* **47,** 9507–9509 (2011).
17. Mor, G. K., Varghese, O. K., Paulose, M., Ong, K. G. & Grimes, C. A. Fabrication of hydrogen sensors with transparent titanium oxide nanotube-array thin films as sensing elements. *Thin Solid Films* **496,** 42–48 (2006).
18. Pan, D. Y. *et al.* C-axis preferentially oriented and fully activated TiO_2 nanotube arrays for lithium ion batteries and supercapacitors. *J. Mater. Chem. A* **2,** 11454–11464 (2014).
19. Wang, J. G., Zhang, P., Li, X., Zhu, J. & Li H. X. Synchronical pollutant degradation and H_2 production on a Ti^{3+}-doped TiO_2 visible photocatalyst with dominant (001) facets. *Appl. Catal. B* **134–135,** 198–204 (2013).
20. Acevedo-Peña. P., Carrera-Crespo, J. E., González, F. & González, I. Effect of heat treatment on the crystal phase composition, semiconducting properties and photoelectrocatalytic color removal efficiency of TiO_2 nanotube arrays. *Electrochim. Acta*, **140,** 564–571 (2014).
21. Wu, J. M., Song, X. M., Ma, L. X. & Wei, X. D. Hydrothermal growth of multi-facet anatase spheres. *J. Cryst. Growth* **319,** 57–63 (2011).
22. Wu, X., Chen, Z. G., Lu, G. Q. & Wang, L. Z. Nanosized anatse TiO_2 single crystals with tunable exposed (001) facets for enhanced energy conversion efficiency of dye-sensitized solar cells. *Adv. Funct. Mater.* **21,** 4167–4172 (2011).
23. Xiang, Q. J., Yu, J. G. & Jaroniec, M. Tunable photocatalytic selectivity of TiO_2 films consisted of flower-like microspheres with exposed {001} facets. *Chem. Commun.* **47,** 4532–4534 (2011).
24. Han, X. G., Kuang, Q., Jin, M. S., Xie, Z. X. & Zheng, L. S. Synthesis of titania nanosheets with high percentage of exposed (001) facets and related photocatlytic properties. *J. Am. Chem. Soc.* **131,** 3152–3153 (2009).
25. Zaban, A., Aruna, S. T., Tirosh, S., Gregg, B. A. & Mastai, Y. The effect of preparation condition of TiO_2 colloids on their surface structures. *J. Phys. Chem. B* **104,** 4130–4133 (2000).
26. Lazzeri, M., Vittadini , A. & Selloni, A. Structure and energetics of stoichiometric TiO_2 anatse surfaces. *Phys. Rev. B*, **63,** 1–9 (2001).
27. Lazzeri, M. & Selloni, A. Strss-driven reconstruction of an oxide surface: the anatase TiO_2 (001)- (1×4) surface. *Phys. Rev. Lett.* **87,** 1–4 (2001).
28. Herman, G. S., Sievers, M. R. & Gao, Y. Structure determination of the two-domain (1×4) anatase TiO_2 (001) surface. *Phys. Rev. Lett*. **84,** 3354–3357 (2000).
29. Gong, X. Q. & Selloni, A. Reactivity of anatase TiO_2 nanoparticles:The role of the minority (001) surface. *J. Phys. Chem. B* **109,** 19560–19562 (2005).
30. Kennedy, G. C. Pressure-volume-temperature relations in water at elevated temperature and pressures. *Am. J. Sci.* **248,** 540–564 (1950).
31. Yang, H. G. & Zeng, H. C. Control of nucleation in solution growth of anatase TiO_2 on glass substrate. *J. Phys. Chem. B* **107,** 12244–12255 (2003).
32. Yin, H. B. *et al.* Hydrothermal synthesis of nanosized anatase and rutile TiO_2 using amorphous phase TiO_2. *J. Mater. Chem.* **11,** 1694–1703 (2001).
33. Kim, W. C., Suh, S. P., Choi, M. J., Kang, Y. S. & Kang, Y. S. Fabrication of $SrTiO_3$-TiO_2 heterojunction photoanode with enlarged pore diameter for dye-sensitized solar cells. *J. Mater. Chem. A* **1,** 11820–11827 (2013).
34. Lu, K. & Wang, J. T. Crystal growth during crystallization of amorphous alloys. *J. Cryst. Growth* **94,** 448–454 (1989).
35. Lu, K., Wang, J., T. & Wei, W. D. A new method for synthesizing nanocrystalline alloys. *J. Appl. Phys.* **69,** 522–524 (1991).

36. Paramasivam, I., Macak, J. M. & Schmuki, P. Photocatalytic activity of nanotube TiO$_2$ layers loaded with Ag and Au nanoparticles. *Elctrochem. Commun.* **10,** 71–75 (2008).
37. Yang, H. S., Tan, Z. M., Liu, Y., Ma. Z. X. & Zhang, L. Hierarchical wall formation of titanium oxide nanotube arrays using anodic oxidation. *IEEE. Trans. Nanotech.* **12,** 1037–1041 (2013).
38. Yu, J. G., Dai, G. P. & Huang, B. B. Fabrication and characterization of visible-light-driven plasmonic photocatalyst Ag/AgCl/ TiO$_2$ nanotube arrays. *J. Phys. Chem. C* **113,** 16394–16401 (2009).

Acknowledgements

Author Contributions

J.D. and H.S.Y. conceived the concept and experiment. J.D. carried out the sample preparation and part of materials characterization and part of photocatalytic measurement. Z.N.H. participated in part of materials synthesis. J.H., Z.X., B.Z. and S.Z.K. participated in part of materials characterization. J.D. and H.S.Y. co-wrote the paper. All author discussed the results.

Additional Information

Supplementary information accompanies this paper at http://www.nature.com/srep

Competing financial interests: The authors declare no competing financial interests.

How to cite this article: Ding, J. *et al.* Low-temperature synthesis of high-ordered anatase TiO$_2$ nanotube array films coated with exposed {001} nanofacets. *Sci. Rep.* **5**, 17773; doi: 10.1038/srep17773 (2015).